



Since January 2020 Elsevier has created a COVID-19 resource centre with free information in English and Mandarin on the novel coronavirus COVID-19. The COVID-19 resource centre is hosted on Elsevier Connect, the company's public news and information website.

Elsevier hereby grants permission to make all its COVID-19-related research that is available on the COVID-19 resource centre - including this research content - immediately available in PubMed Central and other publicly funded repositories, such as the WHO COVID database with rights for unrestricted research re-use and analyses in any form or by any means with acknowledgement of the original source. These permissions are granted for free by Elsevier for as long as the COVID-19 resource centre remains active.

# Human Intestinal Defensin 5 Inhibits SARS-CoV-2 Invasion by Cloaking ACE2

Cheng Wang,<sup>1,\*</sup> Shaobo Wang,<sup>2,\*</sup> Daixi Li,<sup>3,\*</sup> Dong-Qing Wei,<sup>4,5</sup> Jinghong Zhao,<sup>2</sup> and Junping Wang<sup>1</sup>

<sup>1</sup>State Key Laboratory of Trauma, Burns and Combined Injury, Institute of Combined Injury of PLA, Chongqing Engineering Research Center for Nanomedicine, College of Preventive Medicine, Third Military Medical University, Chongqing, China; <sup>2</sup>Department of Nephrology, Xinqiao Hospital, Third Military Medical University, Chongqing, China; <sup>3</sup>Institute of Biothermal Science and Technology, University of Shanghai for Science and Technology, Shanghai, China; <sup>4</sup>State Key Laboratory of Microbial Metabolism, Shanghai-Islamabad-Belgrade Joint Innovation Center on Antibacterial Resistances, Joint Laboratory of International Cooperation in Metabolic and Developmental Sciences, Ministry of Education and School of Life Sciences and Biotechnology, Shanghai Jiao Tong University, Shanghai, China; and <sup>5</sup>Peng Cheng Laboratory, Shenzhen, China

Severe acute respiratory syndrome coronavirus-2 (SARS-CoV-2) emerged recently and caused a coronavirus disease 2019 (COVID-19) outbreak worldwide. Angiotensin-converting enzyme-2 (ACE2) is the main receptor of SARS-CoV-2 S1 and mediates viral entry into host cells.<sup>1</sup> In humans, ACE2 is remarkably abundant on the membrane of lung alveolar epithelial cells and enterocytes.<sup>2</sup> Human intestinal epithelium encompasses approximately 200 m<sup>2</sup> of surface area and is conceivably susceptible to SARS-CoV-2; however, the occurrence of intestinal symptoms is lower than that of respiratory symptoms as a whole,<sup>3</sup> indicating that enterocytes are actually not as easily infected by SARS-CoV-2 as expected. We explored the underlying reason.

## Methods

Intermolecular interaction was determined by biolayer interferometry. Molecular dynamic simulation was performed on a ZDOCK server at Peng Cheng Laboratory. SARS-CoV-2 S1 binding and S pseudovirions entry to targeted cells were investigated by immunofluorescence microscopy, Western blot, and luciferase assay. The significant differences (*P*) were calculated by SPSS 25.0 (IBM Corp, Armonk, NY). More details are shown in the [Supplementary Methods](#).

## Results

### Interaction Between Human Defensin-5 (HD5) and ACE2

HD5, the most abundant  $\alpha$  defensin specifically secreted by intestinal Paneth cells, is in contact with ACE2 on the membrane of enterocytes ([Supplementary Figure 1A](#)). The affinity of HD5 binding to ACE2 was 76.2 nM ([Figure 1A](#)), whereas no association signal was observed for HD5<sub>RED</sub> and another intestinal  $\alpha$  defensin HD6 ([Supplementary Figure 1B and C](#)). In ileal fluid, the content of HD5 is quantified to 6 to 30  $\mu$ g/mL (1.67–8.37  $\mu$ M). Such a high content of HD5 allows an interaction with ACE2 before SARS-CoV-2 lands to enterocytes, although the affinity of SARS-CoV-2 S1 binding to ACE2 is higher than that of HD5 binding to ACE2 ([Figure 1B](#)). Actually, biolayer interferometry-based blocking assay revealed that HD5 preincubation weakened the binding of SARS-CoV-2 S1 to ACE2 ([Figure 1C](#)).

We then investigated the ACE2 blocking by HD5 using molecular dynamic simulation, in which HD5 was docked onto the ligand-binding domain (LBD) of ACE2. After 20 ns of simulation, the complex conformation kept stable with minor residue fluctuations ([Supplementary Figure 1D](#)). The free binding energy of HD5 interacting with LBD was –1866.53 kJ/mol, which was much higher than that of HD5 docking onto SARS-CoV-2 receptor-binding domain (163.24 kJ/mol, [Supplementary Figure 1E](#)). Driven by the potent intermolecular interaction, HD5 attached LBD and cloaked Thr<sup>7</sup>, Gln<sup>24</sup>, Asp<sup>30</sup>, and Lys<sup>31</sup> on  $\alpha$ -helix 1 and Tyr<sup>83</sup> on loop 2 ([Figure 1D](#)).

### Inhibition of HD5 Against SARS-CoV-2 Invasion

Confocal microscopy observed that SARS-CoV-2 S1 largely adhered to the surface of human intestinal epithelium Caco-2 cells in the absence of HD5 after 1 hour of co-incubation ([Figure 1E](#)). When cells were preincubated with 100  $\mu$ g/mL of HD5 for 15 minutes, the recruitment of SARS-CoV-2 S1 was dramatically reduced. Western blot supported that HD5 protected cells from the adherence of SARS-CoV-2 S1 in a dose-dependent manner ([Figure 1F](#)). Notably, SARS-CoV-2 S1 pretreated with HD5 was still efficient to contact Caco-2 ([Supplementary Figure 2A](#)). Furthermore, SARS-CoV-2 S pseudovirions containing pLenti-GFP and dual-luciferase reporter system<sup>4</sup> were used to determine the influence of HD5 on viral entry. Cells infected by the pseudovirions produced green fluorescent protein and the fluorescence signal in the cytoplasm was visibly reduced in the cells pretreated with HD5 ([Supplementary Figure 2B](#)). Luciferase assay confirmed that HD5 significantly inhibited entry of SARS-CoV-2 S

\*Authors share co-first authorship.

**Abbreviations used in this paper:** ACE2, angiotensin-converting enzyme-2; COVID-19, coronavirus disease 2019; HD5, Human Defensin-5; LBD, ligand-binding domain; SARS-CoV-2, severe acute respiratory syndrome coronavirus-2.

 Most current article

© 2020 by the AGA Institute  
0016-5085/\$36.00

<https://doi.org/10.1053/j.gastro.2020.05.015>

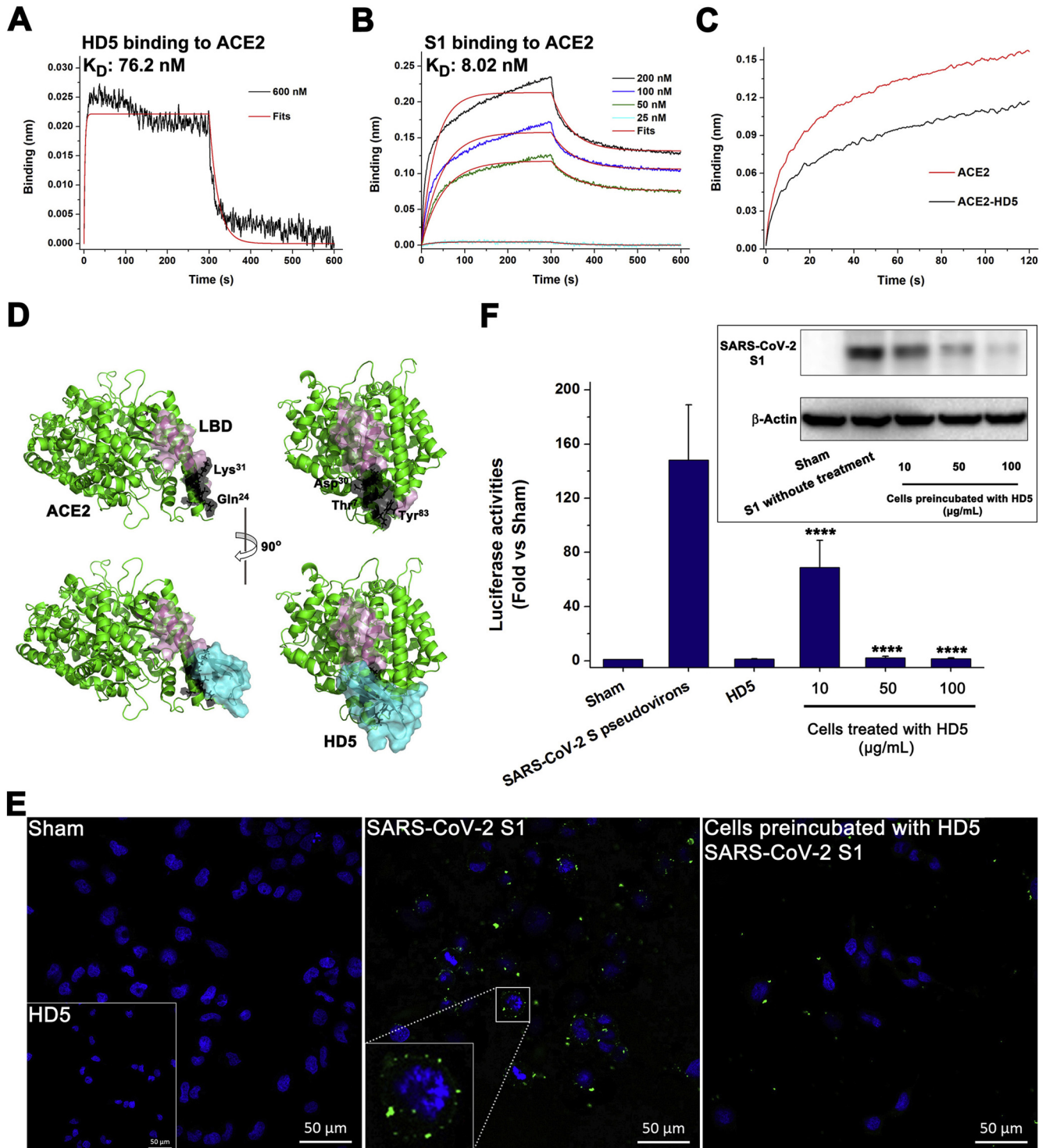


pseudovirions to cells at concentrations as low as 10  $\mu\text{g}/\text{mL}$  (Figure 1F).

peptides, including HD5, which is a lectin-like peptide able to bind lipids and glycosylated proteins.<sup>5</sup> In this study, we found a structure-dependent interaction between HD5 and ACE2. The binding of HD5 to ACE2 cloaked several sites in LBD, among which Asp<sup>30</sup> and Lys<sup>31</sup> are crucial for SARS-CoV spike to bind ACE2.<sup>6</sup> Accordingly, SARS-CoV-2 S1 binding and S pseudovirions entry to enterocytes were inhibited by HD5 (Supplementary Figure 2C). To our knowledge this is the first

### Discussion

Intestinal epithelium encounters trillions of microorganisms, including various viruses. To cope with the microbial threat, intestinal cells have evolved to produce antimicrobial



study demonstrating the innate defense function of human intestine against SARS-CoV-2.

Our finding is a reasonable explanation to the clinical phenomenon that few intestinal symptoms are observed in patients with COVID-19.<sup>3</sup> Because of the deficiency in HD5, patients receiving small intestine transplantation or suffering from inflammatory bowel diseases such as the Crohn's disease, might be more susceptible to SARS-CoV-2 than healthy individuals.<sup>7</sup> HD5 also inhibited SARS-CoV-2 S pseudovirions entry to human renal proximal tubular epithelial cells (Supplementary Figure 2D), demonstrating an extensive protection of HD5. For the shortage of effective drugs to prevent and treat COVID-19, we think that it may be a useful strategy to increase the content of HD5 in vivo by oral administration, as we recently described.<sup>8</sup>

## Supplementary Material

Note: To access the supplementary material accompanying this article, visit the online version of *Gastroenterology* at [www.gastrojournal.org](http://www.gastrojournal.org), and at <https://doi.org/10.1053/j.gastro.2020.05.015>.

## References

1. Lan J, et al. *Nature* 2020;581:215–220.
2. Du M, et al. *Gastroenterology* 2020;158:2298–2301.
3. Huang C, et al. *Lancet* 2020;395:497–506.
4. Ou X, et al. *Nat Commun* 2020;11:1620.
5. Wang C, et al. *J Med Chem* 2015;58:3083–3093.
6. Han DP, et al. *Virology* 2006;350:15–25.
7. Hodson R. *Nature* 2016;540:S97.
8. Zhao G, et al. *Biomater Sci* 2019;7:2440–2451.

Received April 30, 2020. Accepted May 5, 2020.

### Correspondence

Address correspondence to: Junping Wang, State Key Laboratory of Trauma, Burns and Combined Injury, Institute of Combined Injury of PLA, Chongqing Engineering Research Center for Nanomedicine, College of Preventive Medicine, Third Military Medical University, Chongqing, 400038, China. e-mail: [wangjunping@tmmu.edu.cn](mailto:wangjunping@tmmu.edu.cn); Jinghong Zhao, Department of Nephrology, Xinqiao Hospital, Third Military Medical University, Chongqing, 400037, China. e-mail: [zhaojh@tmmu.edu.cn](mailto:zhaojh@tmmu.edu.cn); or Dong-Qing Wei, State Key Laboratory of Microbial Metabolism, Shanghai-Islamabad-Belgrade Joint Innovation Center on Antibacterial Resistances, Joint Laboratory of International Cooperation in Metabolic and Developmental Sciences, Ministry of Education and School of Life Sciences and Biotechnology, Shanghai Jiao Tong University, Shanghai, 200030, China. e-mail: [dqwei@sjtu.edu.cn](mailto:dqwei@sjtu.edu.cn).

### Acknowledgments

We thank Prof Lilin Ye and Dr Xiangyu Chen (Institute of Immunology, PLA, Third Military Medical University) for instructing the pseudovirions entry assay. We appreciate Dr Liting Wang, Dr Wei Sun, and Dr Yi Huang (Biomedical Analysis Center, Third Military Medical University) for the assistance in laser confocal experiment.

Shown as Preprint: bioRxiv 2020.03.29.013490; doi: <https://doi.org/10.1101/2020.03.29.013490>

### CRedit Authorship Contributions

Cheng Wang, PhD (Funding acquisition: Equal; Investigation: Lead; Writing – original draft: Lead). Shaobo Wang, MS (Data curation: Lead; Investigation: Lead). Daixi Li, PhD (Data curation: Equal; Funding acquisition: Equal; Investigation: Equal; Writing – original draft: Supporting). Dong-Qing Wei, PhD (Conceptualization: Equal; Funding acquisition: Equal; Methodology: Lead; Supervision: Equal). Jinghong Zhao, PhD (Conceptualization: Equal; Funding acquisition: Equal; Supervision: Equal; Validation: Lead). Junping Wang, PhD (Funding acquisition: Lead; Supervision: Lead; Validation: Lead; Writing – review & editing: Lead).

### Conflict of interest

The authors disclose no conflicts.

### Funding

This work was supported by grants from the National Natural Science Foundation of China (Nos. 81725019, 81703395, 51776130 and 61832019), the program for scientific and technological innovation leader of Chongqing (CQYC201903084), and the Key Research Area Grant 2016YFA0501703 of the Ministry of Science and Technology of China.

**Figure 1.** HD5 binds to ACE2 and inhibits SARS-CoV-2 S1 binding and S pseudovirions entry to enterocytes. (A) Binding kinetics for HD5 and ACE2 loaded on streptavidin (SA) biosensors. Fits of the data to a 1:1 binding model are shown with red dashes. Times for association and dissociation are both 300 seconds. (B) Binding kinetics for SARS-CoV-2 S1 and ACE2 immobilized on SA biosensors. SARS-CoV-2 S1 is prepared in PBS with concentrations of 200, 100, 50, and 25 nM. (C) Biolayer interferometry-based ACE2 blocking experiment. The binding signals of 100 nM SARS-CoV-2 S1 to ACE2 coated with 600 nM HD5 are recorded for 120 seconds. (D) Stereoview of the cloak of HD5 on LBD. HD5 colored cyan is composed of 32 residues constrained by three disulfide bonds, displaying as a three-stranded antiparallel  $\beta$ -sheet conformation in steric. Residues in LBD (pink) cloaked by HD5 are colored black. (E) Immunofluorescence microscopy revealing the protection of HD5 on Caco-2 exposed to SARS-CoV-2 S1. SARS-CoV-2 S1 adhering to the cell surface is probed by a goat anti-rabbit Alexa Fluor 488 antibody (Green). Nuclei are stained using DAPI (blue). The embedding graph in sham group shows cells treated with HD5. The region of interest in SARS-CoV-2 S1-treated group is magnified in the embedding graph. (F) Luciferase assay. The experiment was conducted in triplicate and repeated three times in different days. Results are shown as mean  $\pm$  standard deviation. Welch test indicated the differences among the groups excluding the sham group ( $F = 52.15$ ,  $P = 1.51 \times 10^{-9}$ ). LSD test showed that, compared with the control group without HD5 treatment ( $n = 9$ ; 148.2 (27.5%)), Caco-2 cells preincubated with HD5 for 1 h at concentrations of 10  $\mu\text{g}/\text{mL}$  ( $n = 9$ ; 68.88 (28.95 %); \*\*\*\*,  $P = 3.23 \times 10^{-10}$ ), 50  $\mu\text{g}/\text{mL}$  ( $n = 9$ ; 2.25 (47.07 %); \*\*\*\*,  $P = 2.89 \times 10^{-18}$ ), and 100  $\mu\text{g}/\text{mL}$  ( $n = 9$ ; 1.59 (37.69 %); \*\*\*\*,  $P = 2.48 \times 10^{-18}$ ) were less sensitive to SARS-CoV-2 S pseudovirions invasion. The embedding graph shows the protein bands of SARS-CoV-2 S1 binding to Caco-2 treated with HD5.  $\beta$ -actin is the reference.



## Supplementary Methods

### Peptide Synthesis

HD5 (3582.3 D, 96% purity), fluorescein isothiocyanate (FITC)-HD5 (4084.5 D, 90.1% purity), HD6 (DEFS-008B, 3707.6 D, 95.7% purity), and HD5<sub>RED</sub> (3588.2 D, 96.2% purity) were prepared by the Chinese Peptide Company (Hangzhou, Zhejiang Province, China).<sup>1,2</sup>

### Immunofluorescence Microscopy

The ileum samples obtained from a healthy donor underwent enteroscopy.<sup>1</sup> The experiment was approved by the Third Military Medical University Institutional Review Board. Caco-2 and HK-2 cells obtained from the cell bank of the Chinese Academy of Sciences (Shanghai, China) and cultured in Dulbecco's modified Eagle's medium (DMEM; Gibco, Thermo Fisher Scientific, Shanghai, China) containing 10% fetal bovine serum (FBS, Gibco) were seeded into a 12-well plate with sterile glass slides at a density of  $2 \times 10^5$  cells per well. A primary anti-ACE2 rabbit polyclonal antibody (1:100, 10108-T24; Sino Biological, Beijing, China) and a goat anti-rabbit secondary antibody (A0516; Beyotime, Shanghai, China) were used to stain ACE2. The coating of HD5 on Caco-2 was analyzed by incubating 50  $\mu\text{g}/\text{mL}$  of FITC-HD5 with cells at 37 °C for 15 minutes.

To evaluate the inhibitive effect of HD5 on SARS-CoV-2 S1 binding to intestinal epithelium, Caco-2 cells were preincubated with 100  $\mu\text{g}/\text{mL}$  of HD5 at 37 °C for 15 minutes, followed by an addition of 8  $\mu\text{g}/\text{mL}$  of S1 (40591-V08H; Sino Biological). Co-incubation was further performed at 4 °C for 1 hour. A primary anti-spike rabbit monoclonal antibody (1:100, 40150-R007; Sino Biological) and a goat anti-rabbit secondary antibody (Alexa Fluor 488; Thermo Fisher Scientific) were used to stain SARS-CoV-2 S1. In pseudovirions experiments, Caco-2 and HK-2 were preincubated with 100  $\mu\text{g}/\text{mL}$  of HD5 at 37 °C for 1 hour, followed by an addition of 200  $\mu\text{L}$  of SARS-CoV-2 S pseudovirions. The cell supernatant was replaced with DMEM containing 10% FBS after 10 hours. The production of green fluorescent protein in cytoplasm was observed after 12 hours. Nuclei were stained with 2-(4-amidinophenyl)-6-indolecarbamide dihydrochloride (DAPI, C1002; Beyotime). A Zeiss (Oberkochen, Germany) LSM 780 NLO confocal microscope was used to observe the cells.

### Biolayer interferometry (BLI)

The bindings of HD5 and SARS-CoV-2 S1 to ACE2 (10108-H02H; Sino Biological) were measured using Forte Bio's "Octet Red 96" BLI (Pall Life Sciences, New York, NY). Biotinylated ACE2 obtained with a biotinylation kit (Genemore, Shanghai, China) was immobilized on streptavidin biosensors. Association and dissociation, 300 seconds for each, were performed at a shaking speed of 1000 rpm. The results were processed using Fortebio Data Analysis 7.0 software. The equilibrium dissociation constant ( $K_D$ ) was

generated by a 1:1 fitting model. BLI-based blocking assay repeated twice on different days was conducted by monitoring the binding of SARS-CoV-2 S1 to ACE2 pretreated with HD5. ACE2 immobilized on streptavidin biosensors was incubated with 600 nM HD5 for 300 seconds at 30 °C. Afterward, the signal of 100 nM SARS-CoV-2 S1 binding to ACE2 was recorded for 120 seconds.

### Molecular Dynamic Simulation

Molecular dock between HD5 (Protein Data Bank: 1ZMP<sup>3</sup>) and the LBD of ACE2 (Protein Data Bank: 6ACG<sup>4</sup>) and the following IRaPPA re-ranking were performed on the ZDOCK server.<sup>5</sup> The Gromacs 2020 software package,<sup>6</sup> AMBER99SB-ILDN force field, and TIP3P water model were applied for all simulations with a time step of 2 fs. First, 1000-step minimization was carried out. Then, for full relaxation, four 1-ns pre-equilibration simulation with restrained coordinates of the atoms belonging to the heavy atoms, main chain, backbone, and C- $\alpha$ , respectively, were performed step by step. Finally, each of 5 production simulations with isothermal-isobaric (NPT) ensemble at 1 atm and 298 K was performed for 20 ns, in total 100 ns. The binding free energy was calculated within 500 snapshots sampled every 10 ps from the final 5 ns trajectory by adopting the molecular mechanics-Poisson-Boltzmann surface area method with g\_mmpbsa procedure for Gromacs.<sup>7</sup>

### Western Blot

Caco-2 cells were seeded into a 6-well plate at a density of  $1 \times 10^6$  cells per well and cultured overnight. Cells preincubated with different concentrations of HD5 (10, 50, and 100  $\mu\text{g}/\text{mL}$ ) at 37 °C for 15 minutes were exposed to 20  $\mu\text{g}/\text{mL}$  of His-tag-containing SARS-CoV-2 S1 at 4 °C for 1 hour. After washing 3 times with PBS, cells were collected and lysed. A total of 25  $\mu\text{g}$  of each protein sample is resolved by 10% sodium dodecyl sulfate-polyacrylamide gel electrophoresis. A primary anti-His-tag mouse monoclonal antibody (1:1000, AF5060; Beyotime) and a goat anti-mouse secondary antibody (A0216; Beyotime) were used to detect SARS-CoV-2 S1.  $\beta$ -actin determined by a mouse monoclonal antibody (1:1000, AA128; Beyotime) was a reference. This assay was repeated twice on different days.

### Luciferase Assay

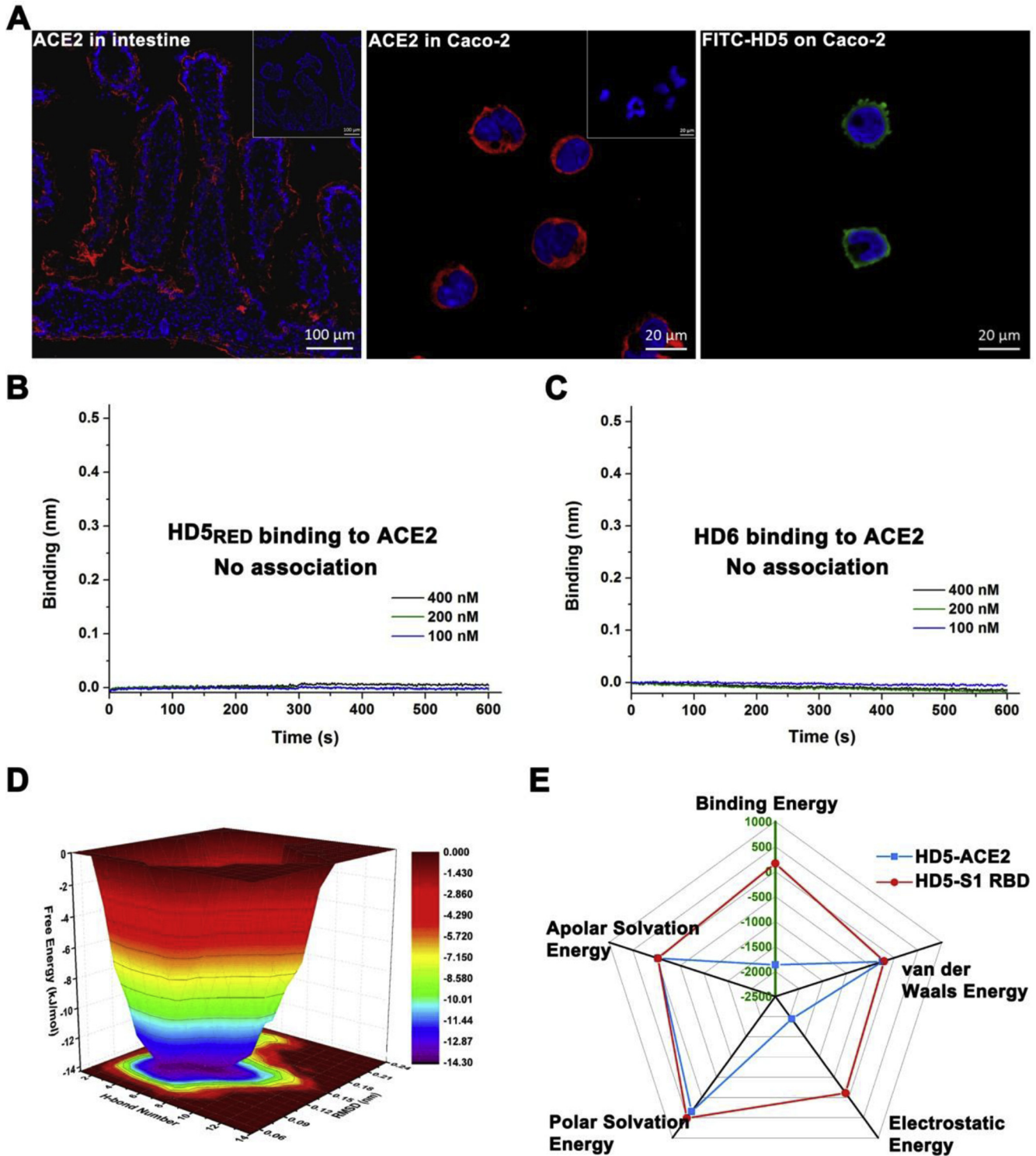
Caco-2 cells were seeded into a 96-well plate at a density of  $5 \times 10^3$  cells per well and cultured overnight. Cells preincubated with 10, 50, and 100  $\mu\text{g}/\text{mL}$  of HD5 at 37 °C for 1 hour were exposed to 200  $\mu\text{L}$  of SARS-CoV-2 S pseudovirions for 10 hours. The dual-luciferase reporter-containing SARS-CoV-2 pseudovirions received from Prof Qian was constructed as recently described.<sup>8</sup> Cells were washed and lysed after 12 hours of post-inoculation in DMEM containing 10% FBS. The transduction efficiency of pseudovirions was determined by measuring the luciferase activity using a dual-luciferase reporter assay system (E1910; Promega, Beijing, China). The experiments were conducted in triplicate and repeated 3 times.

### Statistical Analysis

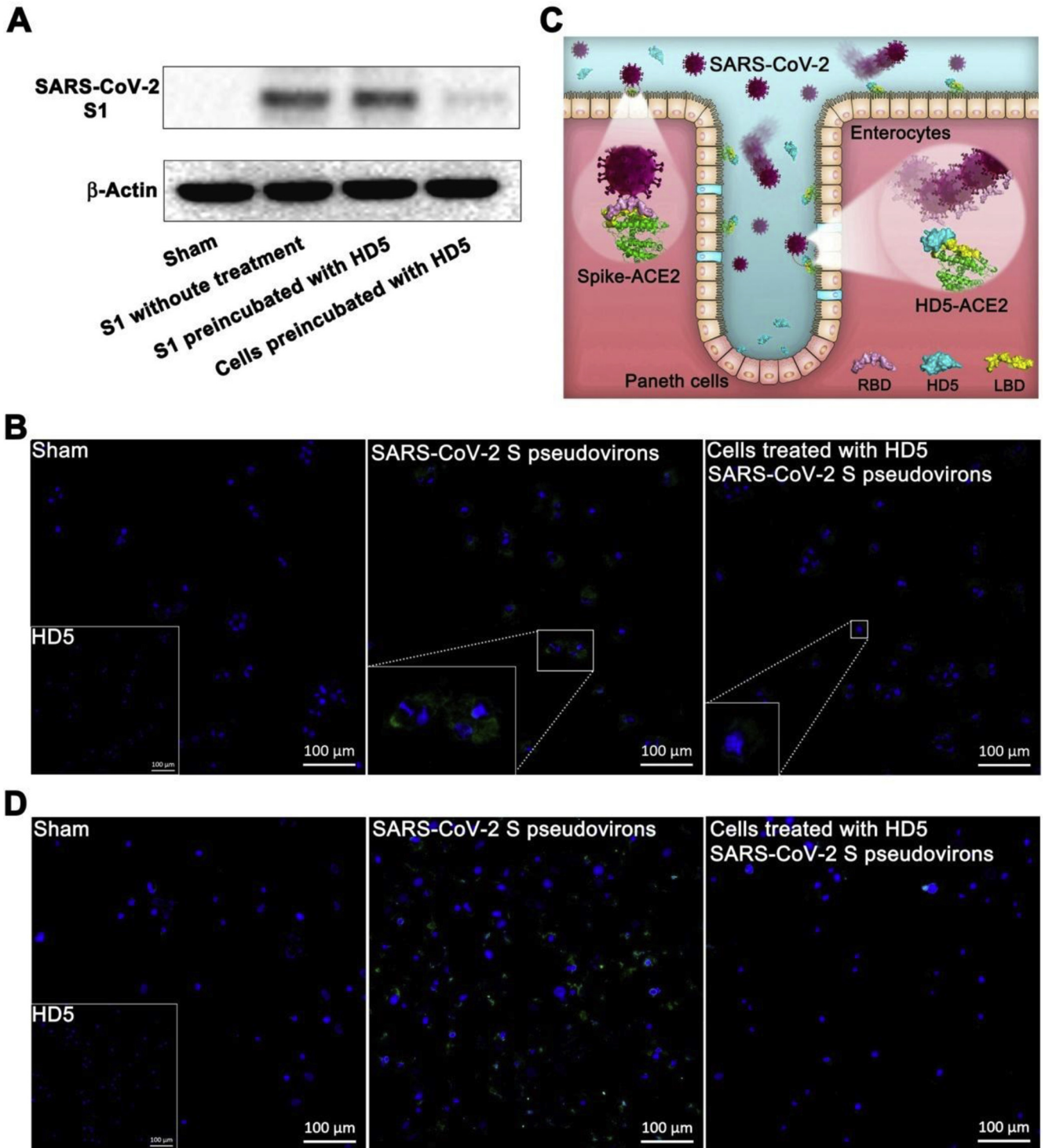
For the disparity in the average luciferase activities differences between the groups, descriptions were expressed by means (coefficients of variation). Comparison of luciferase activities among groups excluding the sham group was performed by Welch test (extension of analysis of variance) because of unequal variances and coefficients of variation. Multiple comparisons were conducted by least significance difference test. The significant differences (*P*) were calculated by SPSS 25.0. A *P* value less than .05 was defined as statistically significant.

### Supplementary References

1. Wang C, et al. *Sci Rep* 2016;6:22875.
2. Wang C, et al. *Antimicrob Agents Chemother* 2018; 62:e01504–e01517.
3. Szyk A, et al. *Protein Sci* 2006;15:2749–2760.
4. Song W, et al. *PLOS Pathogens* 2018;14:e1007236.
5. Pierce BG, et al. *Bioinformatics* 2014;30:1771–1773.
6. Abraham MJ, et al. *SoftwareX* 2015;1-2:19–25.
7. Kumari R, et al. *J Chem Inf Model* 2014;54:1951–1962.
8. Ou X, et al. *Nat Commun* 2020;11:1620.



**Supplementary Figure 1.** Bindings of peptides to ACE2. (A) Immunofluorescence displaying the locations of ACE2 (red) and FITC-HD5 (green) in human intestinal villus and enterocytes. The embedding graphs are the results of control groups. (B) Kinetics for HD5<sub>RED</sub> binding to ACE2 loaded on AR2G biosensors activated by EDC and s-NHS. Fits of the data to a 1:1 binding model are shown with red dashes. (C) Kinetics for HD6 binding to ACE2 loaded on AR2G biosensors. (D) The deep free-energy well of HD5 docking onto the LBD of ACE2. The x-axis is the H-bond number. The y-axis is the root mean square deviation of backbone atoms of HD5. The z-axis is the free-energy landscape of HD5. (E) Energies of HD5 binding to ACE2 and SARS-CoV-2 S1-receptor-binding domain excluding the entropy effect.



**Supplementary Figure 2.** Western blot and immunofluorescence microscopy revealing the protection of HD5 on cells against SARS-CoV-2 invasion. (A) Western blot. Shown are the protein bands of SARS-CoV-2 S1 binding to Caco-2. HD5 preincubation had less of an effect on SARS-CoV-2 S1 binding to ACE2. (B) Immunofluorescence revealing the inhibition of HD5 on SARS-CoV-2 S pseudovirions entry to Caco-2 cells. The embedded graph in the sham group shows cells treated with HD5. The regions of interest in pseudovirions- and HD5-treated groups are magnified. (C) Schematic illustration of the HD5-mediated host innate defense against SARS-CoV-2. Paneth cell-secreted HD5 binds to ACE2 abundant on the intestinal epithelium, lowering viral entry by cloaking the LBD. (D) Inhibition of HD5 on SARS-CoV-2 S pseudovirions entry to human renal proximal tubular epithelial HK-2 cells. The embedded graph in the sham group shows cells treated with HD5.